Macromolecular Chemistry and Physics

Macromolecular Chemistry and Physics
www.mcp-journal.de

RESEARCH ARTICLE OPEN ACCESS

Editor's Choice

Analyzing the Chemical Stability of Bio-Based Polyamide Resins via Solubility Parameters, NMR Spectroscopy and Capillary Electrophoresis

Kash A. Bhullar[1] | Richard Wuhrer[2] | Patrice Castignolles[1,3] | Marianne Gaborieau[1,4]

[1]Australian Centre For Research on Separation Science (ACROSS), School of Science, Western Sydney University, Parramatta, Australia | [2]Advanced Materials Characterisation Facility (AMCF), Western Sydney University, Parramatta, Australia | [3]Institut Parisien De Chimie Moléculaire, Equipe Chimie des Polymères, Sorbonne Université, Paris, France | [4]Karlsruhe Institute of Technology (KIT), Polymer Materials, Institute For Chemical Technology and Polymer Chemistry, Karlsruhe, Germany

Correspondence: Patrice Castignolles (patrice.castignolles@sorbonne-universite.fr) | Marianne Gaborieau (marianne.gaborieau@kit.edu)

Received: 30 April 2025 | **Revised:** 29 August 2025 | **Accepted:** 2 September 2025

Funding: This research was supported by the International Material and Technology Pty Ltd (Imatech, Warwick J. Rule scholarship). Australian Department of Education, Skills and Employment (Research Training Program). Imatech and Western Sydney University (Partnership Grant in Early Project Stages and Academic Development Plan). Agence Nationale de la Recherche (ANR, 3DBIOBASED project).

Keywords: capillary electrophoresis | chemical degradation | Hansen parameters | nuclear magnetic resonance (NMR) spectroscopy | polyamide resin

ABSTRACT

Chemical stability is a key property for polymeric hot-melt adhesives (HMAs) used in industrial settings. The chemical stability of an HMA and its polyamide base resin (obtained from bio-based dimer acids) is assessed after immersion in various solvents. Visual observation and gravimetry show that they resist alkaline conditions better than acidic conditions and are susceptible to dispersion in organic solvents. The organic solvents' impact can be predicted using Hansen parameters. Infrared (FTIR) and solid-state NMR spectroscopies confirm the degradation of the polyamide resins and HMA at the molecular level. Solution-state NMR allows the identification of the type of degradation, such as aromatic substitution. Aromatics and vinylics (from the dimer acid) are quantified with solution-state NMR, including benchtop NMR. The precision of the quantification does not depend on the sensitivity of the instrument but rather on the user-dependent data treatment. The degradation occurs via amide hydrolysis, leading to chain scission, without imide formation. Degradation does not affect the relative amount of vinylics but surprisingly affects that of the aromatics. Free-solution capillary electrophoresis (CE) allows the detection and separation of the most hydrophilic degradation products, including monomers, during the degradation in highly acidic or alkaline conditions without any sample preparation.

1 | Introduction

Rubbers, such as hot-melt adhesives used to repair conveyor belts on mining or other industrial sites, consist of a base resin (such as polyamide) mixed with additives and suffer from gradual deterioration and breakages due to use [1]. They are exposed to heat, sunlight, moisture, oxygen, or other chemicals (organic solvents, organic acids, aqueous acid [2], and alkaline solutions). Plasticization, swelling, and possibly chemical degradation occur when solvent molecules diffuse into the polymer bulk, affecting mechanical properties, durability, structural integrity, and adhesive properties [3]. Identification of the chemical nature and structure of the starting material and degradation products is generally mandatory, especially in terms of compatibility and effects on the surrounding environment, for example, to avoid water pollution [4–6]. To develop superior hot-melt adhesive

formulations based on polyamide resins, it is crucial to evaluate and understand the chemical degradation and the degradation products for improving the product stability under the service conditions and the product's effect on the environment.

Polyamide resins utilized in hot-melt adhesive formulations have been synthesized from diamines such as alkyl, aromatic, oligo(propylene oxide) [7], piperidinyl-based diamine, and oligo(*N*-ethyl amine) (i.e., diethylenetriamine and triethylenetetramine) [8], and bio-based comonomers [9–11]. The bio-based comonomers are sourced from renewable resources such as mixtures of fatty acids, obtained, for example, from wood pulp and castor oil, and are named dimer acids. Dimer acids are complex mixtures of mostly diacids together with some monoacids and triacids [12]. The polyamide resins studied in this work have been previously assessed to be obtained from dimer acids and oligo(propylene oxide) diamines by attenuated total reflectance Fourier transform infrared (ATR-FTIR) and nuclear magnetic resonance (NMR) spectroscopies [7]. These polyamide resins are also sometimes named "specialty nylons" [13], although they differ in their molecular structures (being very heterogeneous copolymers) and crystalline structures from regular nylons. Thermal degradation [14], aging [15], and irradiation [15] of polyamides have been studied to establish the mechanisms of degradation and effects on mechanical properties. However, only a few reports [16–18] have focused on chemical stability and degradation products of polyamide resins in very corrosive acidic, acidic aqueous, alkaline, and non-aqueous conditions. The assessment of chemical stability is standardized (ASTM: D543-14 [19]) with specific requirements including temperature, humidity, sample size, and a range of chemicals. The degradation is quantified through the mass change in the investigated samples and not in terms of degradation products. The standard from ASTM International (formerly the American Society for Testing and Materials) aims at evaluating the structural damage to the polymeric material, not the environmental impact of its degradation.

The separation and characterization of degradation products at the molecular level requires suitable analytical techniques: [20, 21] robust techniques have to withstand highly acidic or alkaline conditions with highly dispersed sample forms (such as molecules, macromolecules, nanoparticles, to microparticles). This analysis is typically carried out by size-exclusion chromatography (SEC), mass spectrometry (MS), and NMR spectroscopy in the literature [20]. SEC suffers from poor reproducibility in general [22, 23], especially in the case of polyamides due to poor solubility, as well as adsorption of polyamides and degradation products onto the SEC stationary phase [24, 25]. Coupling liquid chromatography with other separation or detection methods, either online (e.g., electrospray-ionization (ESI) MS, FTIR, or NMR spectroscopy) or offline (e.g., matrix-assisted laser desorption/ionization with time of flight (MALDI-ToF) MS) has allowed the compositional analysis of oligomers and polymers [20, 26–29]. However, all MS techniques are limited in analyzing high molecular weight synthetic polymers because of the number of different ions arising from the molecular weight distribution and low molecular weight oligomers dominating the spectra [20, 27]. Pyrolysis-gas chromatography is a popular method used for structural analysis in polymer degradation studies; however, it provides indirect information [20, 30]. Thermogravimetry-FTIR is also used to investigate polymer degradation; however, it only provides information on the evolved gases from thermal degradation and mass loss [31].

NMR spectroscopy is a powerful and robust analytical tool routinely used for structural characterization and elucidation of materials (e.g., polymers) [32]. Solution-state NMR was applied to the structure elucidation [33–36] or to study the degradation [36] of several types of polyamide nylons (6; 6,6; 6,9; 6,10; 6,12; and copolymers). NMR spectroscopy was also applied to the structure elucidation of dimer acids [37] and of derived polyamide resins [7]; however, to our knowledge, it has never been applied to quantify the degradation of these resins. ATR-FTIR spectroscopy reveals information on functional groups in solid and liquid samples without requiring sample modification [38]. It is heavily supported by commercial databases covering an array of small molecules, macromolecules, coatings, films, fibers, and inorganic compounds for identification purposes [39]. ATR-FTIR has previously been used to monitor the kinetics of polymerization of dimer acid [40], as well as to confirm the composition of the resulting polymer [10, 41].

Free-solution capillary electrophoresis (CE) is widely used in biopolymers analysis [42] but not much in materials science [43]. It is a high-resolution separation technique that separates ionized analytes through an electric field within a capillary filled with only a background electrolyte (no stationary phase) [44]. This robust analysis technique allows the study of unfavorable or adversely contaminated samples without the need for sample preparation such as filtration or centrifugation, as seen for partially solubilized polymers [45], hardly soluble synthetic polypeptides [46], aggregates, degraded plant fibers [47], and ethanol fermentation by yeast broths [48].

The first aim of this study is to assess the chemical stability of an HMA and its base resin in different chemical environments. This was done through visual observation and gravimetry of HMA and base resin exposed to different solvents. The second aim is to elucidate the degradation mechanisms of the HMA in different chemical environments. The composition of degraded products was investigated by ATR-FTIR, solid-state, and solution-state NMR spectroscopy. The third aim is to test whether CE is a suitable separation technique to investigate polyamide degradation. The composition of the liquid phase after degradation was investigated by CE and solution-state NMR spectroscopy.

2 | Results and Discussion

2.1 | Samples Presentation

The polyamide resins, BaseResin1 and BaseResin2, studied in this work were obtained from dimer acids (derived from tall oil) and oligo(propylene oxide) diamines (see Figure 1 for indicative chemical structures). Their structure was previously assessed in our team by ATR-FTIR and NMR spectroscopies [7]. The hot-melt adhesive HMA was formulated from one of BaseResin1 with 0.01% carbon black. ^{1}H and ^{13}C NMR spectra of BaseResin1 in $CDCl_3$, a solvent in which it is expected to dissolve and not chemically degrade, are shown in Figures 3 and 4.

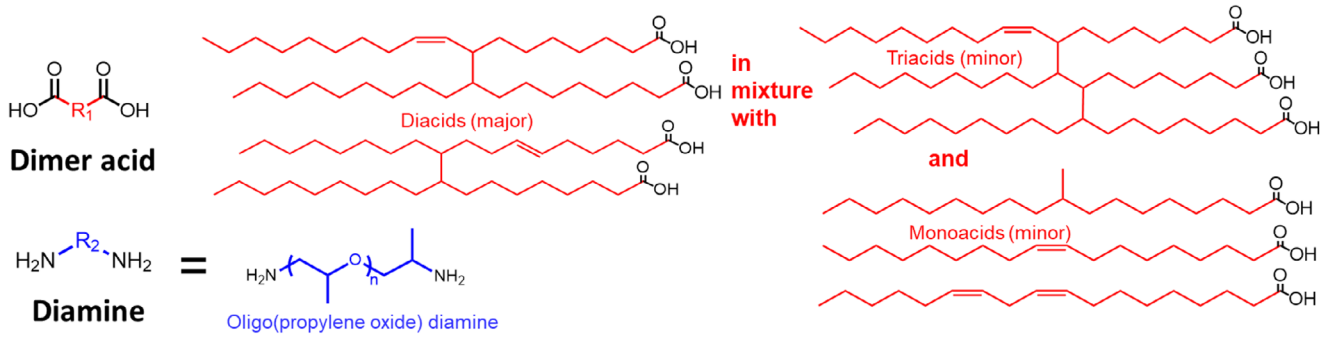

FIGURE 1 | Indicative chemical structures of the dimer acid and oligo(propylene oxide) diamine of the polyamide resin of the present work. Aromatic functional groups were observed in the dimer acid, but their exact structure was not elucidated.

2.2 | Visual Observations and Gravimetry

Chemical resistance tests are used to assess the ability of polyamides and polyamide-based HMAs to withstand exposure to acids, alkalis, aqueous and non-aqueous solvents according to the standard ASTM D543-14 (Standard Practices for Evaluating the Resistance of Plastics to Chemical Reagents) [19]. Some samples prepared in differing conditions (HMA mass, solvent volume, immersion times) are referred to as non-ASTM samples (see Section 4.2). The chemical stability of the polyamides was assessed with visual observation and gravimetry according to this standard (Tables S3–S5 and Figures S1–S11). The resulting liquids and solid samples were also characterized with (solution- and solid-)state NMR (Section 2.3), and CE (Section 2.4) to elucidate the degradation mechanism and the nature of chemicals in the liquids.

HMA samples immersed for seven days in organic solvents (ethanol, diethyl ether, ethyl acetate, acetone, and toluene) swelled with solvent. All liquid phases were clear and still contained the HMA disk on the first day of the study, but changed significantly after the second and seventh days (for visual observations, see Figures S1 and S4). After vacuum drying, very different mass losses were observed (Figure 2a; Table S3), and formed four populations:

- no mass loss with ethanol, water, concentrated or dilute aqueous solutions of sodium hydroxide, of organic acids (formic and acetic acid), of inorganic acids (HCl, H_2SO_4, HNO_3). A mass increase was attributed to some swelling and incomplete drying. Ethanol may have a strong affinity for the polyamide;
- diethyl ether, ethyl acetate, and acetone led to a mass loss between 2 and 22% for both ASTM and non-ASTM tests, and for both HMA and BaseResin1. This is attributed to leaching and evaporation of some additives of the base resin, as well as of some unreacted diamine or monoacid monomers and oligomers, and even possibly a few macromolecules;
- toluene led to a mass loss of 29%. The HMA sample had formed a suspension in toluene. Such a significant mass loss could be explained by a greater leaching of additives, unreacted monomers and oligomers, and even possibly a few macromolecules. This is consistent with the fact that Nylon-12, the most hydrophobic Nylon, swells more in non-polar aromatic hydrocarbons than the other nylons [49];
- pure organic acid, formic and acetic acid, and trifluoroacetic acid (TFA) led to nearly complete mass loss after drying. This can be explained by the degradation of the HMA into volatile compounds and the dissolution of unreacted monomer and oligomers. This includes the hydrolysis of the amide group in the polyamide, leading to the scission of the polymer backbone [50].

Mass loss depends on both solubilities and chemical stabilities. Chemical stability depends both directly and indirectly on the polyamide molecular structure. The functional groups that can react will be discussed in the next sections. The molecular structure also influences the solubility. There are different types of solubilities: [54] the "extraction solubility" is the ability to be dissolved and extracted by a solvent and is relevant for the additives, here non-intentional additives substances (NIAS); the macroscopic solubility, linked to visual observation and transparency; the macromolecular solubility, linked to the concept of critical concentration C* [55]; finally the molecular solubility, linked to solvation [56]. The latter, molecular solubility, is the most relevant to predict chemical stability, but it is currently very little used in the literature [57]. One possibility to predict solubility at the molecular level is based on affinities between functional groups, using solubility parameters for both solutes (here, the polyamides) and solvents. Figure 2a shows the relative mass change of HMA with the Hildebrand [51] (δ_{HB}) and Hansen [52] (δ_t) solubility parameters of the organic solvents. The Hildebrand and Hansen solubility parameters are widely used to measure or predict solvent-solute compatibility. The Hildebrand solubility parameter is dependent on the cohesive energy density, while the Hansen solubility parameter is a combination of three parameters: dispersion, polarity, and hydrogen-bonding. The Hansen and Hildebrand solubility parameters of dimer acid-based polyamide resin are 23 (Figure 2a, blue dashed line) and between 17 and 26 (Figure 2a, pink area), respectively [53]. A comparison of the Hildebrand and Hansen parameters of the polyamide resin and of the solvents causing complete mass loss (i.e., 21–25), showed that the Hansen parameter was a better predictor for this system and could be used for solvents not tested experimentally [19]. The hydrophobic solvents such as heptane, isooctane, and turpentine with δ_t values of 15.3, 14.3, and 16.5 are thus expected to lead to limited mass loss. Carbon tetrachloride,

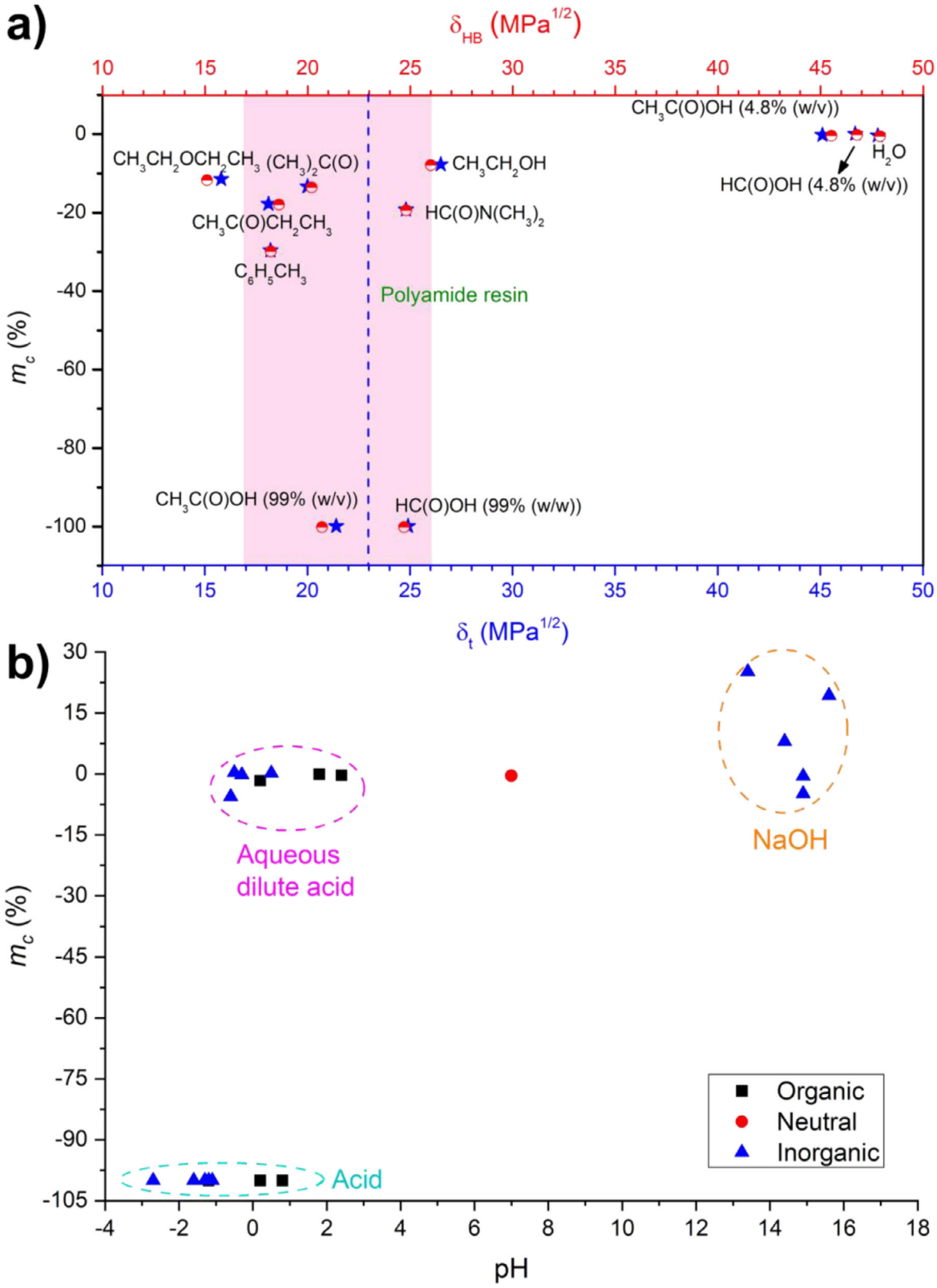

FIGURE 2 | Mass change mc of HMA after immersion and drying against (a) the Hildebrand parameter [51] (δ_{HB}, red symbols) and Hansen parameter [52] (δ_t, blue symbols) of the organic acids and solvents, and (b) the pH of acids, aqueous dilute acids, water, and sodium hydroxide solutions (1, 10, 23, 60% (w/v), as well as 23% (w/v) at 80°C). On (a), the pink area corresponds to the Hildebrand parameter, and the blue dashed line to the Hansen parameter, of polyamide resins [53]. m_c values are listed in Table S3.

ethylene dichloride, and benzene, with δ_t values of 17.7, 20.0, and 18.7 are expected to lead to larger mass loss. The solvents with δ_t values between 21 and 25 are expected to swell and fully disperse the polyamide resin (100% mass loss); these would be for example pyridine, nitrobenzene, cyclohexanol, nitroethane, butanol isomers, acetonitrile, 1-propanol, and methyl glycol with δ_t values of 21.8, 22.2, 22.4, 22.7, 22–23.1, 24.4, 24.5, and 23.5, respectively. The solvents with δ_t values higher than 25 are expected to cause minimal mass change with potential limited mass gain; this would be the case for dimethyl sulfoxide (DMSO, 26.4), and methanol (29.2) [52].

Complete degradation of HMA into volatile compounds or complete dissolution happens only at low pH (Figure 2b) and if the acid can swell the HMA, i.e., if the acid has a Hansen parameter close to that of the polyamide resin. The HMA base resin, BaseResin1, led to similar observations (Figure S10 and Table S4). HMA, however, was completely degraded or solubilized by acetic and formic acid (99% (w/v)), while acetic acid (99% (w/v)) did not physically degrade or macroscopically dissolve a different resin, BaseResin2 (Figure S11 and Table S5), indicating that it may be more hydrophobic or dense (physically crosslinked). Spectroscopic methods were used to obtain information on the degradation products and the degradation mechanism.

2.3 | Mechanism of Polyamide Chemical Degradation

2.3.1 | Solution-State NMR Analysis of Chemically Treated Base Resin and HMA

2.3.1.1 | Qualitative Analysis. The liquid components resulting from HMA immersion, as well as BaseResin1 dispersions in $CDCl_3$, acetic acid-d_4, and acetic acid (99% (w/v)), were analyzed by solution-state NMR to identify degradation products (Figures 3 and 4). HMA chemical treatment conditions were grouped into five broad categories: **alkaline** (NaOH (1, 2.4, 23.3, and 60% (w/w))), **neutral** (water), **aqueous acidic** (formic acid (4.8% (w/v)), acetic acid (4.8% (w/v)), and TFA (4.8% (w/v)), **acidic** (formic acid (99% (w/v)), acetic acid (99% (w/v)) and hydrochloric acid (32% (w/w)), as well as **organic** (diethyl ether, ethyl acetate, toluene, acetone, ethanol, and *N*, *N*-dimethylformamide (DMF). The HMA or BaseResin1 was immersed in the solvent for 7 to 14 days at room temperature (80°C for aqueous NaOH 23%) before an aliquot of the solvent part was prepared for the NMR measurement.

^{1}H and ^{13}C NMR spectra for most aqueous conditions (alkaline, neutral, and acidic) exhibited only solvent signals, consistent with the negligible mass loss in chemical resistance tests (Figure 2b). These NMR results also indicate no significant leaching of water-soluble compounds. For NaOH (23.3% (w/w)) at 80°C, several signals were detected in ^{1}H NMR and a carbonyl signal in ^{13}C NMR (Figures S69 and S70), confirming a reduction in the HMA chemical resistance at higher temperature (Table S3).

^{1}H and ^{13}C NMR spectra for HMA in acidic and organic conditions, as well as for BaseResin1 dispersions, exhibited numerous signals over the whole chemical shift range (Figures 3 and 4). The full signal assignment of ^{1}H and ^{13}C NMR spectra was carried out to identify the chemical structures of the degradation products in these conditions (see top of Figures 3 and 4 for assignment overview, and Tables S6 to S45 for assignment of individual spectra). It was aided by ^{13}C-DEPT-135 (distortionless enhancement by polarization transfer) NMR spectra for carbon degree of substitution (Figures S24, S31, and S46), as well as comparison with ^{1}H and ^{13}C NMR spectra of possible HMA constituents (Figures S73 to S85). Results are presented by type of functional group below.

Carbonyl ^{13}C NMR signals are likely to be from amides (170–175 ppm, carbons bearing no hydrogen according to DEPT-135) of BaseResin1 in $CDCl_3$ and acetic acid (99% (w/v) and $-d_4$) and HMA in organic and acidic conditions. No carboxylic acid signals are detected from the polyamide (175–180 ppm). TFA (99%) had the strongest impact on the macroscopic level. It led to a viscous suspension that could not be analyzed by solution-state NMR (see Section 2.3.2 for solid-state NMR). ^{1}H NMR signals of amides and potentially carboxylic acids (>8 ppm) were only observed as weak signals for BaseResin1 in $CDCl_3$. This is likely due to partial deuteration by $CDCl_3$ and complete deuteration by D_2O added for NMR analysis. For concentrated formic and acetic acids, the large proportion of carboxylic acid groups compared to amide groups (Figures S48 and S50) indicated extensive chain cleavage through amide hydrolysis.

NMR spectra (except for HMA in acidic conditions) exhibited weak vinylic and aromatic signals in the 115–150 ppm range (^{13}C) and 5.3–8 ppm range (^{1}H). Vinylic signals confirm the dimer acid component in the polyamide resin. Aromatic signals come from the base resin but could also originate in additives such as carbon black [7].

NMR spectra exhibited two strong signals in the 70–80 ppm range (^{13}C) and several signals in the 3.1–4.3 ppm range (^{1}H). Signals in this range have been reported to originate in CH_2 of mono or poly(ethylene oxide) components of resins [36, 58, 59]. DEPT-135 NMR spectra showed that signals in the 75–80 ppm range arose from CH_2 and those in the 70–75 ppm range from CH groups, confirming the oligo(propylene oxide) diamine component in the polyamide resin (see Figure 1 for chemical structures) [7]. CH_2 signals in the 39–50 ppm range (^{13}C) and in the 2.5–3.1 ppm range (^{1}H) have been reported to originate in the carbon adjacent to amide (on N side) in polyamide [34, 36]. They were not detected in ^{1}H NMR for the aqueous acidic conditions, possibly due to the interference of a large water signal in the 4.5–5.5 ppm range. Signals in the 20–39 ppm range (^{13}C) and in the 1.2–2.5 ppm range (^{1}H) corresponded mostly CH_2 and a few CH signals. Signals in the 20–10 ppm range (^{13}C) and 0.7–1.2 ppm range (^{1}H) were assigned to methyl groups.

2.3.1.2 | Quantitative Analysis. The polyamide resin contains aromatic and vinylic groups. They were quantified before and after exposure (Figure 5, Table 1). To assess the experimental error, an empirical relation was first used to determine the relative standard deviation (*RSD*) from the signal-to-noise ratio (*SNR*) of a small signal of interest [57]. The *RSD* values determined from *SNR* ranged from 0.01 to 2.3% for the aromatic and vinylic signals (Table S54). The empirical relation is only meaningful when the experimental error primarily comes from the limited signal-to-noise ratio, and it has been shown that a

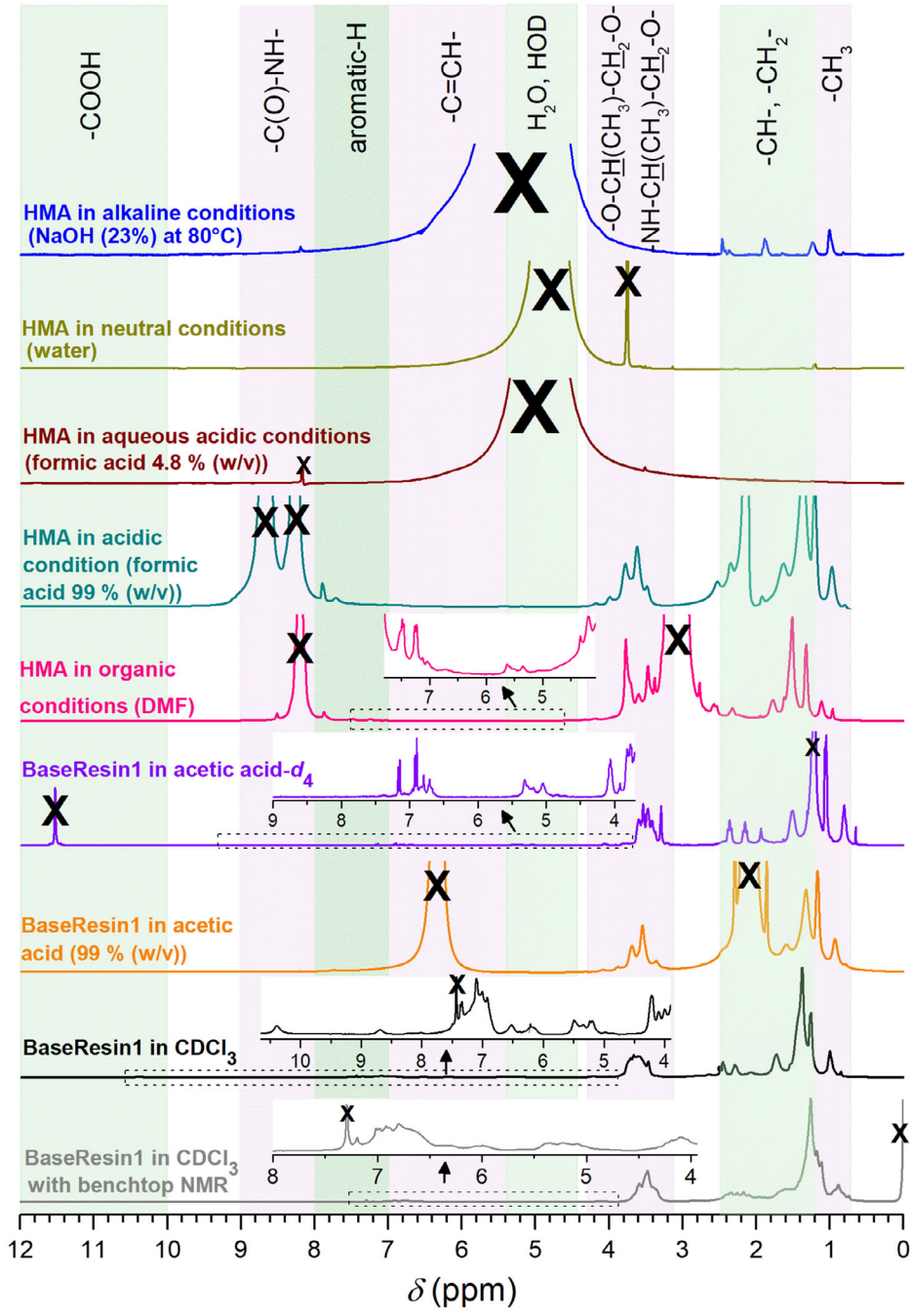

FIGURE 3 | ^{1}H NMR spectra of representative HMA and BaseResin1 dispersions in different conditions, at 300 MHz except for the bottom spectrum (90 MHz). Crosses indicate solvent signals. Exposure was 7 to 14 days at room temperature, except for the alkaline condition (80°C), before an aliquot of the solvent part was prepared for the NMR measurement. For spectra in all solvents, see ^{1}H NMR spectra in figures between S22 and S71.

larger error usually comes from user-dependent data processing (e.g., phasing, baseline correction) [45, 57].

A round-robin test was thus carried out to estimate the experimental error of the integration of different signal ranges in the ^{1}H NMR spectra, with the same set of 7 spectra processed by 4 trained users (Table 1; Figure S85). The aliphatic integral was arbitrarily set to 100 as a reference to compare the weaker integrals of the aromatics and vinylics. No bias from a user was observed, as lower/higher values were distributed among users. The relative standard deviations ranged from 4 to 39 %, allowing for the quantification of the precision of individual aromatic and vinylic fractions (Figure 5). In addition, different hardware was tested for the NMR measurements to estimate accuracy. Benchtop NMR spectroscopy, also referred to as low-field or medium-field NMR spectroscopy, is emerging as a powerful analytical tool in chemometrics, relaxometry, and quality control [60]. In polymer science, compared to high-field NMR spectroscopy, it is an inexpensive and simple alternative for composition analysis [61, 62], for quality control [63], for molecular weight assessment [64], and for monitoring polymer synthesis [65]. It has been used for degradation studies on non-polymer systems such as

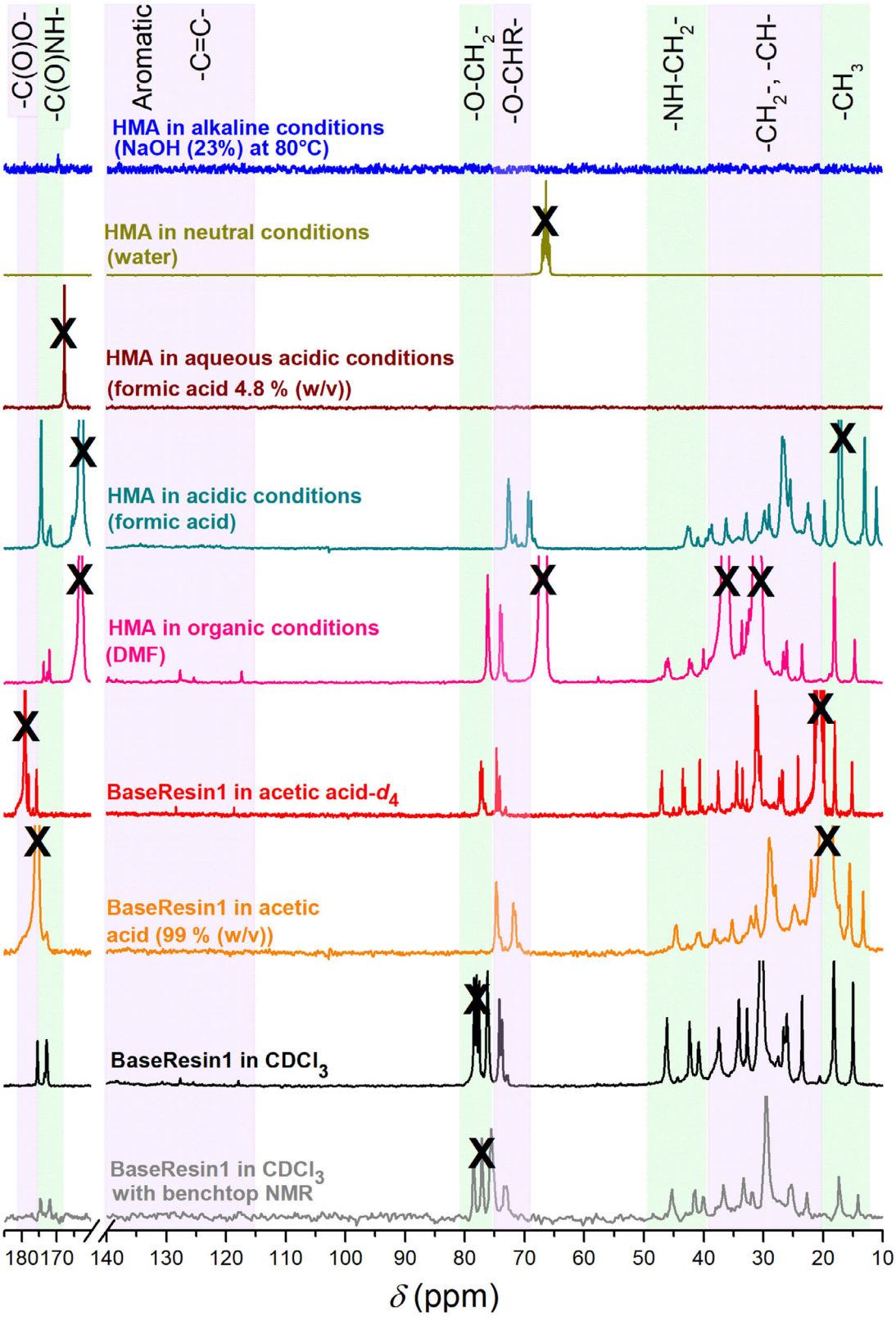

FIGURE 4 | Partial ^{13}C NMR spectra of representative HMA and BaseResin1 dispersions in different conditions, at 75 MHz except for the bottom spectrum (22.5 MHz). Crosses indicate solvent signals. Exposure was 7 to 14 days at room temperature, except for the alkaline condition (80°C), before an aliquot of the solvent part was prepared for the NMR measurement. For spectra in all solvents, see ^{13}C NMR spectra in Figures between S23 and S72.

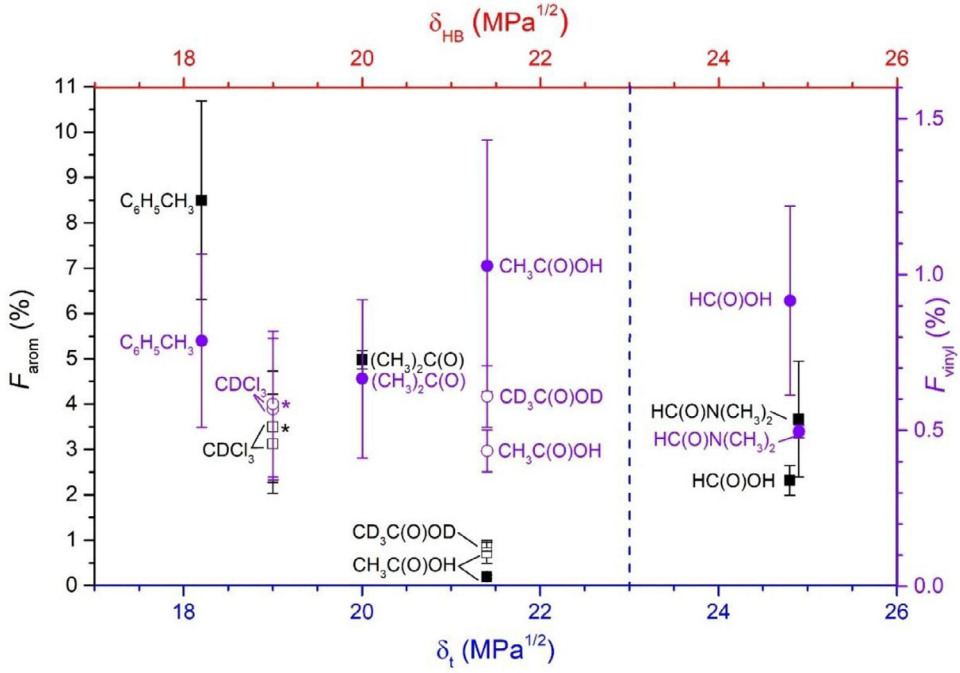

FIGURE 5 | Aromatic (black squares) and vinylic (purple circles) fractions of HMA (full symbols) and BaseResin1 (empty symbols) determined by ^{1}H NMR spectroscopy after immersion against the Hildebrand parameter δ_{HB} [51] and Hansen parameter δ_t. For polyamide resins, the Hansen parameter is indicated by a blue dashed line, while the Hildebrand parameters cover the whole range of the graph [53]. F_{arom} and F_{vinyl} values are listed in Table 1 (except for $CDCl_3$, see Table S54). Asterisks indicate values determined with benchtop NMR. Error bars are the standard deviation determined through the round robin test for each fraction (see Table 1), except for $CDCl_3$ for which the standard deviation (SD) was chosen as the highest SD in the round-robin (35 % for aromatics, 40 % for aliphatics).

persistent organic pollutants [66]. Compared to high-field NMR spectra, ^{1}H and ^{13}C NMR spectra of BaseResin1 in $CDCl_3$ recorded with benchtop NMR exhibit the same signals with slightly reduced resolution in ^{1}H NMR and reduced sensitivity in ^{13}C NMR (Figures 3 and 4; see overlays in Figures S26 and S28, respectively). There was no significant difference between the aromatic (or vinylic) fractions determined with high-field and benchtop NMR in $CDCl_3$, assuming for the RSD the highest value found for that fraction in the round-robin test (Figure 5). The sensitivity was lower for benchtop NMR than for high-field NMR (with *SNR* values lower by a factor of 3.5 to 4.5 for equal numbers of scans, see Table S54), with *SNR* still sufficient to ensure an *RSD* from *SNR* at least 20 times lower than the *RSD* from the round-robin test. Thus, the precision of the aromatic and vinylic fractions was not affected in this work by the limited signal-to-noise ratio, while its accuracy was not affected by the spectrometer but by the user-dependent processing, such as phasing and setting baseline. This also demonstrates the potential of benchtop NMR spectroscopy to assess the composition and monitor the degradation or depolymerization of this class of bio-based polymeric adhesives at a much lower running cost.

The evolution of aromatic or vinylic ^{1}H fractions with the Hildebrand and Hansen parameters was obtained for samples for which ^{1}H NMR spectra were recorded (Figure 5). Note that the corresponding solvents all had Hildebrand parameters in the range of the polyamide resin ones, because no usable NMR data was obtained outside of it due to shim or lock issues or weak signals. Thus, solution-state NMR spectroscopy brings additional information, but on a limited range of samples. No significant difference was observed in the vinylic fraction, while significant differences can be confidently identified in the aromatic fraction, F_{arom}. The decrease in F_{arom} in formic or acetic acid compared to toluene or acetone is, however, likely due to chemical degradation. Aromatic functional groups are typically more chemically resistant than vinylic ones. Rather than aromatic ring breakage, the cause of the decrease in F_{arom} in acidic conditions is thus more likely an increase in substitution of the aromatic rings, causing a decrease in the number of hydrogens directly bound to the rings. In addition, a decreased solvation [56, 67] of the aromatic rings in organic acidic solvents compared to neutral organic solvents could contribute to the decrease in F_{arom}. The ability of aromatic functional groups to perform π-π stacking might explain why their molecular solubility is more affected than that of aliphatics or vinylics in different solvents. Solution-state NMR spectroscopy is thus relevant to assess solubility in that case, but one should be very careful before drawing conclusions about chemical degradation (or synthesis) from it. Chemically treated base resin and HMA were thus investigated with spectroscopy in the solid state.

2.3.2 | Solid-State ATR-FTIR and NMR Analysis of Chemically Treated Base Resin and HMA

BaseResin1 was analyzed by ATR-FTIR spectroscopy before and after immersion in a blend of acetic acid (99% (w/v), 1.2 mL), ethanol (2 mL), and water (1 mL) followed by freeze-drying. It confirmed the polyamide nature of the non-degraded and

TABLE 1 | Integrals of aromatic and vinylic signals obtained for various samples in a round-robin test with 4 users: Individual results (for users U1 to U4), their average (*Av.*, underlined), standard deviation (*SD*), and relative standard deviation (*RSD*). Integrals in each spectrum are arbitrarily scaled to 100 for aliphatics, so that the integrals of aromatic and vinylic signals are equal to F_{arom} and F_{vinyl}. For each spectrum and region, the lowest value is italicized and the highest one is bolded.

Sample	Aromatics integral						Vinylics integral					
	U1	U2	U3	U4	*Av.*	*SD*	*RSD*	U1	U2	U3	U4	*Av.*	*SD*	*RSD*
HMA in DMF	*1.83*	2.46	2.46	**2.53**	2.32	0.33	14%	1.00	*0.68*	**1.31**	*0.68*	0.92	0.30	33%
BaseResin1 in acetic acid-d_4	*0.78*	**1.04**	0.80	0.90	0.88	0.12	14%	*0.51*	0.60	0.58	**0.75**	0.61	0.10	16%
BaseResin1 in acetic acid	0.62	0.73	**1.04**	*0.50*	0.72	0.23	32%	0.40	0.43	**0.53**	*0.38*	0.43	0.07	16%
HMA in toluene	7.78	*6.16*	8.68	**11.38**	8.50	2.19	26%	*0.58*	0.69	0.68	**1.20**	0.79	0.28	35%
HMA in formic acid	2.95	3.56	**5.50**	*2.67*	3.67	1.28	35%	**0.52**	*0.48*	0.50	0.49	0.50	0.02	4.0%
HMA in acetic acid	**0.23**	0.20	0.21	*0.13*	0.19	0.04	23%	0.91	**1.40**	1.29	*0.51*	1.03	0.40	39%
HMA in acetone	**5.12**	5.10	*4.68*	5.03	4.98	0.20	4.1%	*0.41*	0.53	0.73	**0.99**	0.67	0.25	38%

freeze-dried acetic acid (99% (w/v)) degraded BaseResin1 samples through their characteristic bands along with the presence of vinylic components and the existence of a C—O—C bond within both samples (Figure S86; see Table S55 for full signal assignment) [7]. The carbonyl band around 1735 cm^{-1} was reported to change during the degradation of a bio-based polyamide in an accelerated artificial ageing environment (with UV, moisture, temperature), with a shoulder at 1735 cm^{-1} assigned to photo-oxidation into imide [15]. Such a change is not observed in this work (Figure S86, inset), and no imide formation is detected. Due to the inability of ATR-FTIR spectroscopy to differentiate and resolve signals of interest, solid-state NMR spectroscopy was used for the analysis of HMA samples.

HMA was analyzed by solid-state NMR spectroscopy before and after immersion for 7 to 14 days in NaOH (23.3% (w/w) at 80°C) or TFA (97% (w/v) at 25°C) followed by drying of the solid part. ^{1}H MAS (magic-angle spinning) NMR spectra of untreated HMA samples showed limited resolution at room temperature [7]. In this work, the resolution of the dried solid components of degraded HMA was insufficient to observe changes in its structure (Figure 6a, see Figures S87, S89, and S91 for individual spectra). The two resolved signals for HMA and HMA treated with NaOH (23.3% (w/w)) were observed around 1 ppm for the aliphatic signal and 3.5 ppm for the oligo(propylene oxide) signal, while four to five signals were observed for the TFA (97% (w/v)) treated HMA sample, which may have been due to increased molecular mobility of the sample due to degradation (see Tables S56, S58, and S60 for signal assignment). Vinylic and aromatic signals could be identified only in this TFA-treated HMA sample; however, they were severely overlapping with each other and with a more intense signal at 8 ppm (Figures S87). The linewidth in ^{1}H NMR relates to the mobility of the functional groups, i.e., the sharper the signal, the more mobile the functional group, hence the much lower resolution compared to solution-state NMR (see Section 2.3.1). The linewidths of the untreated HMA and NaOH-treated HMA were similar, while the linewidth of TFA-treated HMA was visually narrower. It was expected since degradation would lead to the generation of smaller molecules, which would be more mobile than the polymer backbone. In addition, ^{13}C SPE (single-pulse excitation)-MAS NMR was used to compare samples to address resolution issues faced in ^{1}H MAS NMR.

^{13}C SPE-MAS NMR spectroscopy allowed improved resolution and observation of signals of interest (Figure 6b, see Figures S88, S90, and S92 for individual spectra and Tables S57, S59, and S61 for signal assignment [7]). The ^{13}C SPE-MAS NMR spectra of TFA-treated HMA showed sharper signals and implied the functional groups were more mobile than in the untreated HMA, indicative of chain scission. The detection of the carboxylic group after degradation indicates that the scission is likely by the hydrolysis of the amide group. The ^{13}C CP (cross-polarization)-MAS NMR spectra of TFA-treated HMA and untreated HMA (Figures S93) showed that the TFA-treated HMA was not wholly degraded, as some residual backbone signals were detected. Note that ^{13}C CP-MAS NMR is not as sensitive to small molecules, which are very mobile and are difficult to detect with this method. ^{13}C SPE-MAS can detect all functional groups, typically with a higher resolution and a much lower sensitivity than ^{13}C CP-MAS NMR. Very faint signals detected with ^{13}C SPE-MAS in the vinylic and

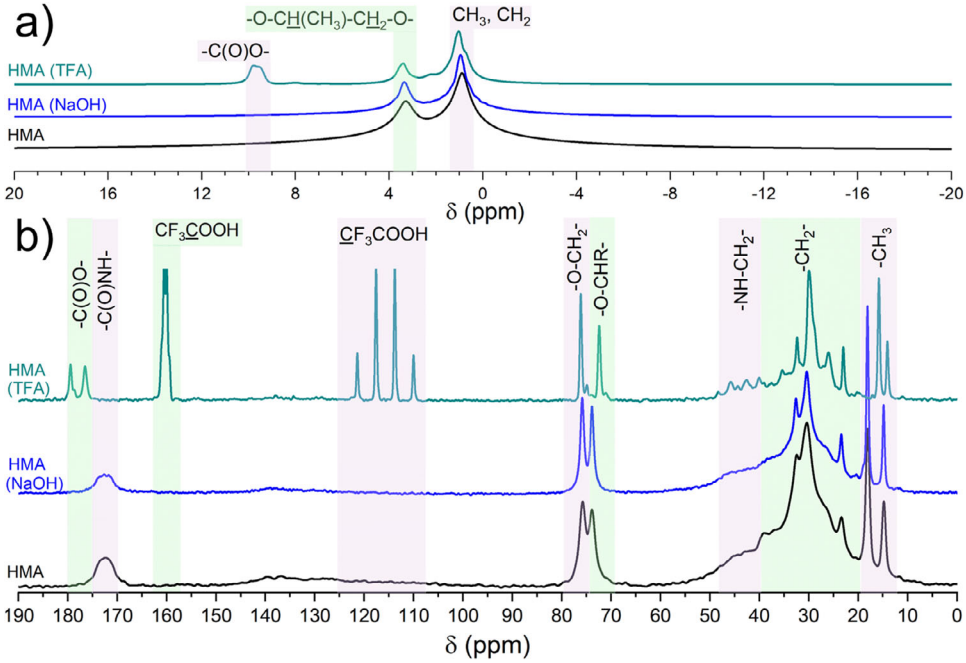

FIGURE 6 | (a) ^{1}H MAS and (b) ^{13}C SPE-MAS NMR spectra of HMA (black), HMA treated with NaOH (23.3% (w/w) by immersion for 7–14 days at 80°C followed by drying) (blue), and HMA treated with TFA (97% (w/v) by immersion for 7–14 days at 25°C followed by drying) (green).

aromatic ranges (signals 2 in Figures S90, S92) could originate in aromatic and vinylic groups or in background signal from the NMR instrument. ^{13}C solution-state NMR exhibited an even higher resolution; however, no aromatic or vinylic signals were detected for this sample, and solubility may be incomplete at the molecular level (Figures S56). A quantitative NMR assessment of the degradation of vinylic and aromatic functional groups would thus need ^{13}C-labelled samples and ^{13}C SPE-MAS NMR. This expensive approach is relevant in fundamental research but not applicable to research and development or quality control.

2.3.3 | HMA Degradation Mechanism

In the present work, both the liquid and the solid phase of the chemical stability study of a polyamide-based HMA exposed to solvents were analyzed using solution-state and solid-state NMR spectroscopy (Sections 2.3.1 and 2.3.2, respectively). This complemented information obtained from visual observation to elucidate the mechanism of degradation of the adhesive. The proposed mechanism (Figure 7) is consistent with earlier reports of degradation mechanisms for other types of polyamides: nylon-like polyamides. Studies focusing on polyamide hydrolysis have reported accelerated polyamide hydrolysis in acidic environments through amine scavenging and acid catalysis [18, 68]. This means that acidic hydrolysis leads to the formation of oligomers of varying sizes, and the rate of hydrolysis is affected by the nature of the diacid and diamine component [69], e.g., a large alkyl group would hinder hydrolysis near an amide bond. These studies reported that small organic acids were able to absorb into the solid polyamide, thus resulting in a lower pH within the polyamide structure, which inhibited the re-polymerization of the broken amide bonds. Overall, it is thought that this mechanism occurs most likely through the free amine groups reacting preferentially with the small organic acids, rather than with larger monomer or polymer acid end groups, thus reducing the equilibrium molecular weight of the degradation product [18, 68].

Organic solvents such as diethyl ether, ethyl acetate, toluene, acetone, ethanol, and DMF were able to form viscous dispersions within a few days visually. Polyamide resins have a very low solubility in these solvents. The organic solvents are not expected to chemically degrade the polymers. The degradation of the HMA samples is thus expected to arise at the macroscopic and macromolecular level rather than at the molecular level. This enabled the general identification of the composition of the polyamide by comparison with a few possible reactants by analysis via solution-state ^{1}H, ^{13}C and ^{13}C DEPT-135 NMR, i.e., dimer acid, alkyl diamine, aromatic diamine, oligo(*N*-alkyl amine) and oligo(propylene oxide) diamine (Figure 1; see Figures S73–S84 and signal assignment Tables S46–S53) [70–72].

The extent of polyamide solubility could be measured through the ability to detect dimer acid alkene functions in solution-state ^{13}C NMR [57], which was observed in all organic solvents, while this was not the case in organic acids, as some alkene would undergo hydrogenation [73]. However, this implied that the polyamide was not highly crosslinked (due to the triacid component of the dimer acid), or it would not be able to form a dispersion. From this, the polyamide composition was confirmed as dimer acid and oligo(alkyl oxide) diamine with small amounts of aromatic or alkyl diamines. Polyamide resins based on dimer acids may include some alkene functions. It was reported that the oligo(alkyl oxide) component of polyamide resins undergoes degradation in concentrated mineral acids such as nitric acid and sulfuric acid, yielding polyglycols and amino alcohols [74], but not in hydrochloric acid since chloride is not a strong enough nucleophile [71, 72]. Upon understanding the polyamide composition, the degradation mechanism could be fully established, building on Figure 7.

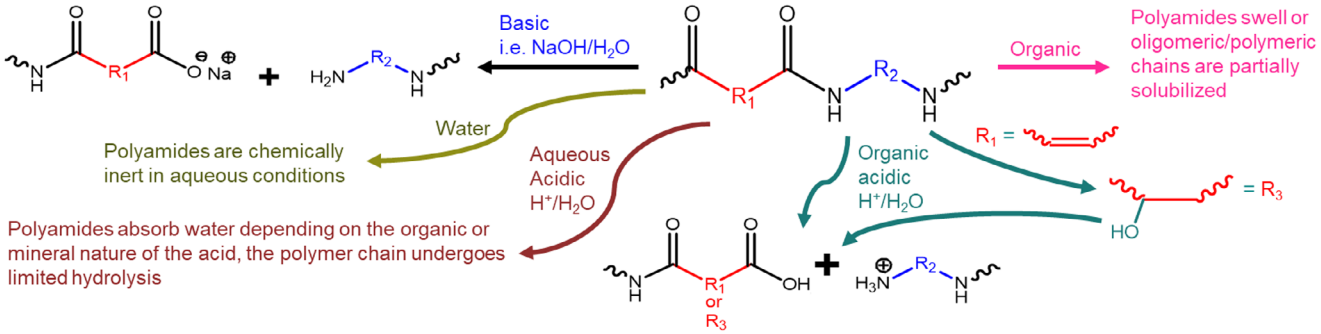

FIGURE 7 | Proposed polyamide degradation scheme in different solvents, based on information obtained from visual observations and NMR spectroscopy.

2.4 | A Capillary Electrophoresis Method to Separate and Detect Hydrophilic Products of Polyamide Chemical Degradation

The chemical degradation of the polyamide resins leads to a range of products with a broad range of hydrophobicity, from highly hydrophobic long-chain-fatty-acid-like products to potential small molecules with carboxylic acid or amine functions. The hydrophilic compounds may be especially relevant in terms of the environmental impact of the degradation. Solution-state NMR measurements did not detect the hydrophilic compounds due to sensitivity or solubility issues. Diluting the degradation products in an excess of aqueous (deuterated) solvent would lead to a large loss of sensitivity, the main weakness of NMR. Drying the degradation dispersion to redissolve in aqueous (deuterated) solvent would lead to inconsistencies in drying the dispersion, depending on the solvent used, and more importantly, an unknown and likely problematic accuracy due to incomplete dissolution of the hydrophilic products, depending on the matrix. Another method is thus being tested to directly separate and detect hydrophilic degradation products: free solution capillary electrophoresis (CE).

CE has been shown to handle the analysis of sample mixtures in complex matrices, including suspended or aggregated macromolecules [45, 46, 48]. From the HMA degradation mechanism, the HMA undergoes degradation in some solvents and leaching in others. The effect of the degraded or leached products can also be detrimental after the stoppage of mining and during mining site restorations. To the best of our knowledge, this is the first time that polyamide degradation products have been analyzed by CE. Unfiltered liquid components of the HMA in formic acid and aqueous NaOH (Figure 8) as well as in acetone (Figures S108–S110, S123,S124), aqueous acetic acid (Figures S125-S125), hydrochloric acid (Figures S128–S130), nitric acid (Figures S131–S133), water (Figures S111–S113, S136–S139) and NaOH (1.1 or 2.4% (w/w), Figures S117–S118, S140–S141) were analyzed on different days to assess whether CE can analyze these types of samples. After injection, the sample is mixed with the aqueous borate buffer due to "mixing by the electric field" [45]. In several cases, repeatable peaks were detected only in the early times (ethyl acetate 7 days, formic acid 7 days), at intermediate times (acetic acid 21 days), or only after long exposure (water 42 and 104 days). In other cases, no peaks were detected (diethyl ether, acetone, aqueous acetic acid, aqueous hydrochloric acid, aqueous sulfuric acid). The latter is consistent with transparent liquids being obtained. The peaks correspond to molecules that are hydrophilic, with some solubility in aqueous borate buffer.

Possible monomers of the polyamide in the HMA, i.e., dimer acid, alkyl diamine, aromatic diamine, and oligo(propylene oxide) diamine, were injected separately for identification purposes (Figures S94–S97, Table S63). The only monomer that may be observed is the diacid of the dimer acid that may be present in the degradation with formic acid and aqueous NaOH. Acid or alkaline solutions may lead to some depolymerization, but the amount of diacid is limited and not persistent, likely due to the poor solubility of the diacid in aqueous solutions. The molecule released with extraction by acetone, ethyl acetate, and toluene (see Section 2.2 and Table S63) might be an additive present in the base resin, but more likely NIAS in the base resin. The long-term leaching observed with water likely consists of different (not identified) molecules.

The electrophoretic mobility distributions of BaseResin1 exposed to highly concentrated acids (hydrochloric acid (32% (w/w)) and acetic acid (99% (w/v))) (Figures S99–S104) showed no significant peaks like those of the HMAs (Figure 8; Figures S128–S130). Hydrophilic products leached or dissolved from HMA are likely not additives from the HMA but come from the polyamide resin.

3 | Conclusion

The polyamide-based HMA and polyamide resins tested in this work, obtained from dimer acid and oligo(propylene oxide) diamine, were exposed to different solvents and highly corrosive conditions commonly found in mining and manufacturing sites. They were strongly resistant to moderately corrosive mineral acids and mineral bases. The fatty acid nature of the composition led to HMA losing structural integrity and swelling in organic solvents. DMF was shown to be particularly efficient at dispersing HMA. Hansen and, to a lesser extent, Hildebrand parameters were shown to be good predictors of the mass change after exposure to organic solvent. No change in chemical stability from the polyamide base resin to HMA was observed; however, a different

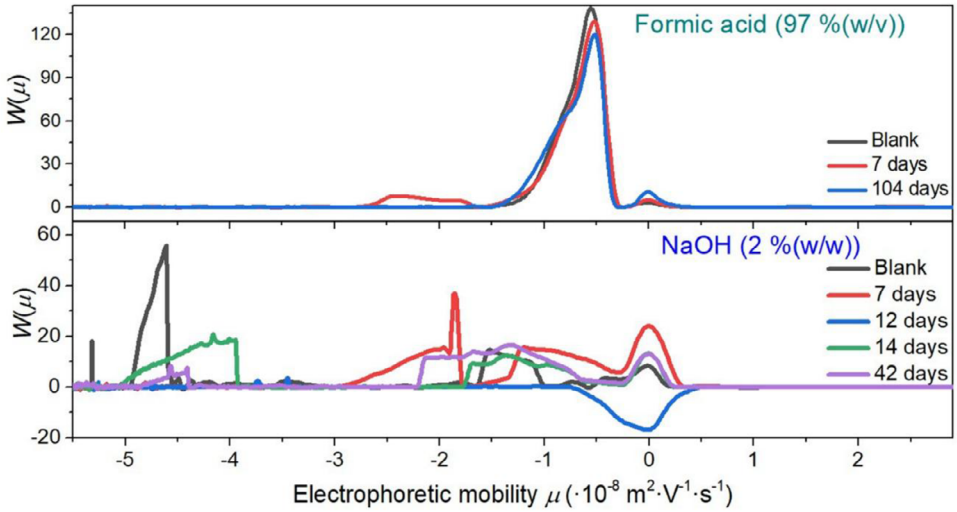

FIGURE 8 | Electrophoretic mobility distributions of the liquid aliquots of non-ASTM study samples in formic acid and aqueous NaOH at various degradation times, as well as from a blank containing only the degradation solvent.

polyamide resin was more resistant to glacial acetic acid than the investigated polyamide resin and HMA. Semi-crystallinity of the polyamide may also affect its chemical resistance.

Solution-state NMR spectroscopy of liquids showed signals even where visually no degradation was observed, indicative of polyamide precursors (diacid and diamine). The signals were important in determining the structure of the degradation products. The error in quantification originates primarily in user-dependent data processing rather than in the instrument sensitivity. The changes in NMR signals highlighted the formation of carboxylic acid and the breakdown of amide, as well as the decrease in vinylic group hydrogens. This may indicate chain-scission via hydrolysis in acidic and basic conditions, as well as oxidation of the dimer acid vinylic bonds in acidic conditions, respectively. Solid-state characterization of the chemically treated HMA samples using ATR-FTIR and NMR spectroscopy confirmed the degradation of the HMA polyamide. The importance of understanding the chemical stability of polyamide and HMA was demonstrated with data suggesting they degrade similarly.

Benchtop NMR spectroscopy was able to resolve signals for a polyamide resin dispersed in $CDCl_3$, with a similar sensitivity for ^{1}H NMR and a lower sensitivity for ^{13}C NMR compared to high-field NMR. While benchtop NMR relaxometry has already proven useful to characterize rubber degradation, such as artificial weathering [75], this work shows that benchtop NMR spectroscopy is powerful enough to characterize rubber degradation at the molecular level. It is applicable in non-deuterated solvents with appropriate solvent suppression techniques like WET (water suppression enhanced through T_1 effects). Benchtop NMR is more affordable than high-field NMR, allowing in-situ monitoring of degradation processes of this class of bio-based polymeric adhesives over several days. This makes solution-state NMR a powerful tool to improve polymers' stability under service conditions.

CE was used for the first time to separate and detect hydrophilic products of degradation. CE proved a robust enough method even in highly acidic conditions. The initial monomers can be detected with this CE method. Depolymerization in acidic or alkaline conditions may be observed, though limited, likely by poor solubility. Different molecules leach into water only after a very long time. Acidic buffer and different detectors could be used, such as conductivity detectors and MS detectors for comprehensive identification. This methodology is applicable to different polymers used on mining or other industrial sites, in particular polyamides and other HMAs. It has the potential to contribute to the environmental impact assessment of polyamide HMAs degradation and allow the analysis of potential contaminants for soil reclamation on mining sites after the conclusion of mining.

4 | Experimental Section

4.1 | Materials

Polyamide resin samples (BaseResin1 and BaseResin2) in pellet form, and HMA samples composed of BaseResin1 (99.9%) along with CarbonBlack1 (0.01%) in molded disk-shaped pellets, were supplied by the company Imatech (Castle Hill, Australia) [7]. BaseResin1 and BaseResin2 were obtained by polycondensation of dimer acid (derived from tall oil) and alkyl diamine. Pripol 1017 dimer acid with monoacid (2%), 1½-mer acid (5%), diacid (78%), and triacid (20%) was provided by Croda Chemicals. Jeffamine D-230 (oligo(propylene diamine), M_n of 230 g mol^{-1}, PED230) was provided by Huntsman Corporation.

All water used in this study was of Milli-Q quality. Acetic acid (glacial, 99% (w/v)), trifluoroacetic acid (TFA, 98% (w/v)), hydrochloric acid (32 and 36% (w/w)) were purchased from Unilab. Boric acid (≥99.5%), formic acid (≥99%), sulfuric acid (95–98% (w/w)), ethanol (≥99%), dimethyl sulfoxide (DMSO, ≥99%), *N*,*N*-dimethylformamide (DMF, ≥99%), acetone (≥99%), ethyl acetate (≥99%), ethanol (≥99%), diethyl ether (≥99%), toluene (≥99%), ethylenediamine (≥99.5%), methanol (≥99%), *N*-(1-naphthylenediamine dihydrochloride) and adamantane (99%) were obtained from Sigma-Aldrich Chemical company.

Sodium hydroxide (≥97.5%, pellets) and nitric acid (68-70% (w/w)) were provided by Ajax Finechem. $CDCl_3$ (99.8% D), 1,4-dioxane-d_8 (dioxane-d_8, 99% D), deuterium oxide (99.9% D), acetic acid-d_4 (99.9% D) and singly ^{13}C-labelled alanines (1-^{13}C, 2-^{13}C, 3-^{13}C; 99%) were obtained from Cambridge Isotope Laboratories, Inc. Sodium borate (200 mM) was prepared from 0.5 M boric acid in water, titrated to pH 9.20 with 10 M sodium hydroxide, and diluted with water [76]. Sodium borate was sonicated for 5 min and filtered with a Whatman (0.2 µm) or Millex GP polyethersulfone syringe filter (0.22 µm) and a plastic syringe before use.

Oxygen was not removed in any of the experiments. Samples were kept in the dark with limited exposure to artificial light.

4.2 | Gravimetry

The chemical resistance of the polyamides and HMA formulation was studied as per ASTM: D543-14 method [19]. The effect of different solvents was studied on the polyamide resin and the HMA samples: organic solvents (DMF, acetone, ethyl acetate, ethanol, diethyl ether, and toluene), a neutral pH solvent (water), acids (formic acid (4.8 and 99% (w/v)), acetic acid (4.8 and 99% (w/v)), TFA (4.8 and 97% (w/v)), hydrochloric acid (24% (w/v) and 32% (w/w)), nitric acid (10.7% (w/v), 48.3% (w/v) and 70% (w/w)) and sulfuric acid (1.7, 18.9 and 97% (w/v) as well as alkalis (NaOH (1, 2.4, 23.3, and 60% (w/w) (see Table S1 for details of solvent preparation and other experimental parameters). In each case, a pre-weighed sample was immersed in the solvents for 7-14 days at room temperature. The sample was then removed, initially dried with pressurized air, then vacuum dried (100 mbar) in an oven at 40°C until its mass was constant. In the case of alkaline solvents, the sample was washed with water before air-drying as per the ASTM method. After drying, the sample was weighed, and the mass change (m_c) was determined using Equation 1.

$$m_c\,(\%) = 100 \cdot \frac{m_f - m_o}{m_o} \tag{1}$$

where m_o is the initial mass before immersion, and m_f is the final mass after drying. Visual observations were performed using a smartphone 5.0 MP camera with white paper as a background.

Some samples were prepared with a smaller size of HMA and volume of solvent, as well as different immersion times (Sections S1.2, S1.3, S2.2, and S2.3); these are named non-ASTM samples in the manuscript.

4.3 | NMR Spectroscopy

NMR spectra were recorded on a Bruker DRX300 spectrometer (Bruker BioSpin Pty Ltd, Sydney), at Larmor frequencies of 300.13 MHz for ^{1}H and 75.48 MHz for ^{13}C, at room temperature (~25°C), unless otherwise specified.

4.3.1 | Solution-State NMR

For degraded HMA samples and BaseResin1, samples were prepared for NMR measurements by adding 50 µL of 1,4-dioxane-d_8 or D_2O to 450 µL of the degraded sample liquid in the ASTM chemical resistance test (7 days or more). BaseResin1 samples were suspended in either acetic acid-d_4 or $CDCl_3$ (ca. 100 g•L^{-1}), and the samples were measured when a visually clear suspension was obtained. ^{1}H, ^{13}C, and ^{13}C-Distortionless Enhancement by Polarization Transfer (DEPT)-135 spectra were recorded with a repetition delay of 7.47, 5, and 9.83 s, respectively, unless otherwise specified, and with number of scans in the range of 256–5120, 4096–75509, and 1553–100859, respectively (see figure captions in Supporting Information for the number of scans of each experiment). A 5-mm dual ^{1}H/^{13}C probe was used. The ^{1}H and ^{13}C chemical shift scales were externally calibrated to the methyl signal of ethanol in D_2O at 1.17 and 17.47 ppm, respectively, unless otherwise specified [77].

The relative standard deviation *RSD* was estimated for selected signals from their signal-to-noise ratio *SNR* using an empirical relation (Equation 2) [57].

$$RSD\,(\%) = \frac{238}{SNR^{1.28}} \tag{2}$$

In a round-robin test, 4 trained users processed the same set of 7 ^{1}H NMR spectra independently. Each user performed a Fourier transform with 0.3 to 5 Hz exponential apodization (same apodization value for all users for a given spectrum), a manual phase correction, a local baseline correction over each of the ranges of interest manually with a cubic spline, followed by an integration over each of the ranges of interest. The ranges of interest were approximately: 7.5–6.5 ppm for aromatics, 4.5–5.7 ppm for vinylics, 0–1.7 ppm for aliphatics. The aromatic and vinylic ^{1}H fractions F_{arom} and F_{vinyl} were expressed as a percentage of aliphatic ^{1}H nuclei using Equation 3:

$$F_{arom}\,(\%) = 100 \cdot \frac{I_{arom}}{I_{aliph}} \quad \text{and} \quad F_{vinyl}\,(\%) = 100 \cdot \frac{I_{vinyl}}{I_{aliph}} \tag{3}$$

where I_{arom}, I_{vinyl}, and I_{aliph} are the integrals of the aromatic, vinylic, and aliphatic signals, respectively. A representative spectrum without and with local baseline corrections is shown in Figure S85.

For comparison, solution-state ^{1}H and ^{13}C NMR spectra of BaseResin1 were recorded with benchtop NMR. BaseResin1 was suspended (100 g L^{-1}) in $CDCl_3$ containing tetramethylsilane (TMS) and measured when a visually clear suspension was obtained. ^{1}H and ^{13}C NMR were recorded on a Spinsolve 90 ULTRA Carbon spectrometer (Magritek, Aachen, Germany), at Larmor frequencies of 90 MHz for ^{1}H and 22.5 MHz for ^{13}C, at room temperature, with repetition delays of 10 and 3.5 s, with 128 and 10,240 scans, respectively. The ^{1}H and ^{13}C chemical shift scales were calibrated to the TMS signal at 0.00 ppm [77].

4.3.2 | Solid-State NMR

A commercial double-resonance, magic-angle spinning (MAS) probe was used with zirconia rotors of 4 mm outer diameter and 3 mm inner diameter. For ^{1}H and ^{13}C single pulse excitation (SPE-MAS) experiments, the 90° pulse was optimized using adamantane. For ^{13}C cross-polarization (CP-MAS) experiments,

power levels were optimized using a mixture of three ^{13}C singly labeled alanines. The ^{1}H and ^{13}C chemical shift scales were externally referenced by setting the CH resonance of adamantane to 1.64 and 38.48 ppm, respectively [78].

NMR spectra of HMA before and after treatment in ASTM conditions with TFA (97% (w/v)) and NaOH (23.3% (w/w)) at 80°C were recorded at 10 kHz MAS. ^{1}H MAS NMR spectra were recorded with a 5.1 µs 90° pulse, a 3 s repetition delay, and 32 scans. ^{13}C SPE-MAS NMR spectra were recorded with a 3.5-8.23 µs 90° pulse, a 3 s repetition delay, with 8192, 7478, and 5012 scans, respectively. ^{13}C CP-MAS NMR spectra were recorded with a 3.5 µs 90° pulse, a 1 ms contact time, and a 3 s repetition delay, with 12288 and 48402 scans, respectively.

4.4 | Attenuated Total Reflection Fourier Transform Infrared Spectroscopy

ATR-FTIR spectra of the non-degraded BaseResin1 and freeze-dried BaseResin1 resin degraded for 35 days by a blend of acetic acid (99% (w/v), 1.2 mL), ethanol (2 mL), and water (1 mL) were recorded with a Bruker Vertex 70 Spectrometer with a 2 cm^{-1} resolution and 64 scans. Good coverage of the ATR window crystal (diamond) was ensured by adjusting the sample position and pressing with a gauge, without prior sample preparation, until a real spectrum showed distinct signals. The background was measured before each measurement. The data were recorded, normalized, and baseline corrected using Bruker OPUS software suite. The data was presented using the software OriginPro 9.0.

4.5 | Capillary Electrophoresis

CE experiments were carried out in bare fused silica capillaries using sodium borate (200 mM, pH 9.2) as a background electrolyte following a published approach [76] (see Section S10 in supporting information for more details). The capillaries and instrument were validated before each session using a well-studied oligoacrylate (Table S62) [79, 80]. Raw data (migration time, intensity) was converted into a weight-distribution of electrophoretic mobility ($W(\mu)$) [81].

Acknowledgements

The authors thank Scott Cheevers, Joel Thevarajah, Russell Eggers, and Imatech for providing samples and useful discussions on conditions in mining sites, as well as Jed Bonne and Joshua Dunn for performing some of the visual tests and capillary electrophoresis measurements. The authors thank Laurel George, Daniel Fanna, and the Advanced Materials Characterisation Facility at Western Sydney University for support and discussions, as well as Morgan Raguideau (Sorbonne université) for his participation in the round-robin test.

Conflicts of Interest

The authors declare no conflicts of interest.

Data Availability Statement

The raw data and processed data required to reproduce these findings are available to download from Mendeley Data https://doi.org/10.17632/m2bs6zzbsj.3

References

1. W. Li, L. Bouzidi, and S. S. Narine, "Current Research and Development Status and Prospect of Hot-melt Adhesives: A Review," *Industrial & Engineering Chemistry Research* 47 (2008): 7524–7532.

2. R. E. Mielke, D. L. Pace, T. Porter, and G. Southam, "A Critical Stage in the Formation of Acid Mine Drainage: Colonization of Pyrite by Acidithiobacillus Ferrooxidans Under pH-neutral Conditions," *Geobiology* 1 (2003): 81–90.

3. B. Deneve and M. E. R. Shanahan, "Physical and Chemical Effects in an Epoxy-resin Exposed to Water-vapor," *Journal of Adhesion* 49 (1995): 165–176.

4. D. Leistenschneider, A. Wolinski, J. G. Cheng, et al., "A Critical Review on the Evaluation of Toxicity and Ecological Risk Assessment of Plastics in the Marine Environment," *Science of the Total Environment* 896 (2023): 164955.

5. New South Wales Government, in *Protection of the Environment Operations Act 1997 No 156* (New South Wales Government, 2019).

6. The European Parliament, Council of the European Union, in *Regulation (EC) No 1272/2008 of the European Parliament and of the Council of 16 December 2008 on Classification, Labelling and Packaging of Substances and Mixtures* (EUR-Lex, 2008).

7. K. A. Bhullar, A. Meinel, K. Maeder, R. Wuhrer, M. Gaborieau, and P. Castignolles, "Advanced Spectroscopy, Microscopy, Diffraction and Thermal Analysis of Polyamide Adhesives and Prediction of Their Functional Properties With Solid-state NMR Spectroscopy," *Polymer Chemistry* 12 (1487): 1487–1497.

8. C. Rossitto, "Polyester and Polyamide High Performance Hot Melt Adhesives," in *Handbook of adhesives* (Chapman & Hall, 1990), 478–498.

9. J. L. J. van Velthoven, L. Gootjes, B. A. J. Noordover, and J. Meuldijk, "Bio-based, Amorphous Polyamides With Tunable Thermal Properties," *European Polymer Journal* 66 (2015): 57–66.

10. E. Hablot, B. Donnio, M. Bouquey, and L. Averous, "Dimer Acid-based Thermoplastic Bio-polyamides: Reaction Kinetics, Properties and Structure," *Polymer* 51 (2010): 5895.

11. X. M. Chen, H. Zhong, L. Q. Jia, et al., "Polyamides Derived From Piperazine and Used for Hot-melt Adhesives: Synthesis and Properties," *International Journal of Adhesion and Adhesives* 22 (2002): 75–79.

12. R. Brutting and G. Spiteller, "Produkte Der Dimerisierung Ungesättigter Fettsäuren XII: Die Dimerisierung von Konjuensäure," *Fett Wissenschaft Technologie-Fat Science Technology* 96 (1994): 445–451.

13. G. Odian, "Step Polymerization," in *Principles of Polymerization* (John Wiley and Sons, Inc., 2004), 39.

14. X. D. Fan, Y. L. Deng, J. Waterhouse, and P. Pfromm, "Synthesis and Characterization of Polyamide Resins From Soy-based Dimer Acids and Different Amides," *Journal of Applied Polymer Science* 68 (1998): 305–314.

15. E. Hablot, A. Tisserand, M. Bouquey, and L. Averous, "Accelerated Artificial Ageing of New Dimer Fatty Acid-based Polyamides," *Polymer Degradation and Stability* 96 (2011): 1097–1103.

16. B. Jacques, M. Werth, I. Merdas, F. Thominette, and J. Verdu, "Hydrolytic Ageing of Polyamide 11. 1. Hydrolysis Kinetics in Water," *Polymer* 43 (2002): 6439–6447.

17. A. Horta, J. Coca, and F. V. Díez, "Degradation Kinetics of Meta- and Para-aromatic polyamides," *Advances in Polymer Technology* 22 (2003): 15–21.

18. S. Hocker, A. K. Rhudy, G. Ginsburg, and D. E. Kranbuehl, "Polyamide Hydrolysis Accelerated by Small Weak Organic Acids," *Polymer* 55 (2014): 5057–5064.

19. ASTM International, in *ASTM D543-14: Standard Practices for Evaluating the Resistance of Plastics to Chemical Reagents* (ASTM International, West Conshohocken, PA, USA, 2014).

20. A. Ghaffar, P. J. Schoenmakers, and S. van der Wal, "Methods for the Chemical Analysis of Degradable Synthetic Polymeric Biomaterials," *Critical Reviews in Analytical Chemistry* 44 (2014): 23–40.

21. A. C. Albertsson and M. Hakkarainen, in *Chromatography for Sustainable Polymeric Materials: Renewable, Degradable and Recyclable*, (Springer, 2008).

22. D. Berek, "Size Exclusion Chromatography—A Blessing and a Curse of Science and Technology of Synthetic Polymers," *Journal of Separation Science* 33 (2010): 315–335.

23. E. Uliyanchenko, S. van der Wal, and P. J. Schoenmakers, "Challenges in Polymer Analysis by Liquid Chromatography," *Polymer Chemistry* 3 (2012): 2313–2335.

24. S. Laun, H. Pasch, N. Longieras, and C. Degoulet, "Molar Mass Analysis of Polyamides-11 and-12 by Size Exclusion Chromatography in HFiP," *Polymer* 49 (2008): 4502–4509.

25. G. Marot and J. Lesec, "Size Exclusion Chromatography of Polyamides," *Journal of Liquid Chromatography* 11 (1988): 3305–3319.

26. E. Reingruber and W. Buchberger, "Analysis of Polyolefin Stabilizers and Their Degradation Products," *Journal of Separation Science* 33 (2010): 3463–3475.

27. C. M. Guttman, K. M. Flynn, W. E. Wallace, and A. J. Kearsley, "Quantitative Mass Spectrometry and Polydisperse Materials: Creation of an Absolute Molecular Mass Distribution Polymer Standard," *Macromolecules* 42 (1695): 1695–1702.

28. T. F. Beskers, T. Hofe, and M. Wilhelm, "Online Coupling of Size-exclusion Chromatography and IR Spectroscopy to Correlate Molecular Weight With Chemical Composition," *Macromolecular Rapid Communications* 33 (1747): 1747–1752.

29. C. Botha, J. Hopfner, B. Mayerhofer, and M. Wilhelm, "On-line SEC-MR-NMR Hyphenation: Optimization of Sensitivity and Selectivity on a 62 MHz Benchtop NMR Spectrometer," *Polymer Chemistry* 10 (2019): 2230–2246.

30. A. Chojnacka, H. G. Janssen, and P. Schoenmakers, "Detailed study of polystyrene solubility using pyrolysis–gas chromatography–mass spectrometry and combination With size-exclusion chromatography," *Analytical and Bioanalytical Chemistry* 406 (2014): 459–465.

31. J. M. Cervantes-Uc, J. V. Cauich-Rodriguez, H. Vazquez-Torres, and A. Licea-Claverie, "TGA/FTIR Study on Thermal Degradation of Polymethacrylates Containing Carboxylic Groups," *Polymer Degradation and Stability* 91 (2006): 3312–3321.

32. T. D. W. Claridge, "Introduction," in *High-Resolution NMR Techniques in Organic Chemistry*, (Elsevier, 2016), 1.

33. R. D. Davis, W. L. Jarrett, and L. J. Mathias, "Solution 13C NMR Spectroscopy of Polyamide Homopolymers (Nylons 6, 11, 12, 66, 69, 610 and 612) and Several Commercial Copolymers," *Polymer* 42 (2001): 2621–2626.

34. B. S. Holmes, W. B. Moniz, and R. C. Ferguson, "NMR study of nylon 66 in solution (proton, carbon-13, and nitrogen-15 NMR using adiabatic J cross polarization)," *Macromolecules* 15 (1982): 129–132.

35. Y. Zhou, W. Xue, Z. Zeng, W. Zhu, and Z. Li, "Amine-terminated Nylon 6/66/1010 (AM-6/66/1010) Used for Hot Melt Adhesives: Synthesis and Properties," *Journal of Adhesion Science and Technology* 29 (2015): 670–677.

36. M. R. Krejsa, K. Udipi, and J. C. Middleton, "NMR Analysis of UV- and Heat-aged Nylon-6,6, 1997," *Macromolecules* 30 (4695): 4695–4703.

37. K. J. Park, M. Kim, S. Seok, Y. W. Kim, and D. H. Kim, "Quantitative Analysis of Cyclic Dimer Fatty Acid Content in the Dimerization Product by Proton NMR Spectroscopy," *Spectrochimica Acta Part A: Molecular and Biomolecular Spectroscopy* 149 (2015): 402–407.

38. S. Prati, E. Joseph, G. Sciutto, and R. Mazzeo, "New Advances in the Application of FTIR Microscopy and Spectroscopy for the Characterization of Artistic Materials," *Accounts of Chemical Research* 43 (2010): 792–801.

39. N. Vasanthan and D. R. Salem, "FTIR Spectroscopic Characterization of Structural Changes in Polyamide-6 Fibers During Annealing and Drawing," *Journal of Polymer Science Part B: Polymer Physics* 39 (2001): 536–547.

40. D. Montarnal, P. Cordier, C. Soulie-Ziakovic, F. Tournilhac, and L. Leibler, "Synthesis of self-healing supramolecular rubbers From fatty acid derivatives, diethylene triamine, and urea," *Journal of Polymer Science Part A: Polymer Chemistry* 46 (2008): 7925–7936.

41. R. F. R. Freitas, C. Klein, M. P. Pereira, et al., "Lower Purity Dimer Acid Based Polyamides Used as Hot Melt Adhesives: Synthesis and Properties," *Journal of Adhesion Science and Technology* 29 (1860): 1860–1872.

42. R. L. C. Voeten, I. K. Ventouri, R. Haselberg, and G. W. Somsen, "Capillary Electrophoresis: Trends and Recent Advances," *Analytical Chemistry* 90 (1464): 1464–1481.

43. I. Desvignes, J. Chamieh, and H. Cottet, "Separation and Characterization of Highly Charged Polyelectrolytes Using Free-solution Capillary Electrophoresis," *Polymers* 10 (2018): 1331.

44. R. Weinberger, "Capillary Zone Electrophoresis: Basic concepts," in *Practical Capillary Electrophoresis*, (Academic Press, 2000), 25.

45. J. J. Thevarajah, J. C. Bulanadi, M. Wagner, M. Gaborieau, and P. Castignolles, "Towards a Less Biased Dissolution of chitosan," *Analytica Chimica Acta* 935 (2016): 258–268.

46. H. Miramon, F. Cavelier, J. Martinez, and H. Cottet, "Highly Resolutive Separations of Hardly Soluble Synthetic Polypeptides by Capillary Electrophoresis," *Analytical Chemistry* 82 (2010): 394–399.

47. J. D. Oliver, M. Gaborieau, E. F. Hilder, and P. Castignolles, "Simple and Robust Determination of Monosaccharides in Plant Fibers in Complex Mixtures by Capillary Electrophoresis and High Performance Liquid Chromatography," *Journal of Chromatography A* 179 (2013): 179–186.

48. J. D. Oliver, A. T. Sutton, N. Karu, et al., "Simple and Robust Monitoring of Ethanol Fermentations by Capillary Electrophoresis," *Biotechnology and Applied Biochemistry* 62 (2015): 329–342.

49. V. R. Sastri, "Engineering Thermoplastics: Acrylics, Polycarbonates, Polyurethanes, Polyacetals, Polyesters, and Polyamides," in *Plastics in Medical Devices*, (William Andrew Publishing, 2010), 121.

50. B. G. Achhammer, F. W. Reinhart, and G. M. Kline, "Mechanism of the Degradation of Polyamides, 1951," *Journal of Applied Chemistry* 1 (1951): 301–320.

51. A. F. M. Barton, "Section 8.3: Single-component donor-parameters," in *CRC Handbook of Solubility Parameters and Other Cohesion Parameters*, (Taylor & Francis, 1991), 271.

52. A. F. M. Barton, "Section 5.9: Hansen Parameters," in *CRC Handbook of Solubility Parameters and Other Cohesion Parameters* (Taylor & Francis, 1991), 95.

53. A. F. M. Barton, "Determination of polymer cohesion parameters," in *CRC Handbook of Solubility Parameters and Other Cohesion Parameters* (Taylor & Francis, 1991), p. 406.

54. N. Najjoum, N. Grimi, M. Benali, M. Chadni, and P. Castignolles, "Extraction and Chemical Features of Wood Hemicelluloses: A Review," *International Journal of Biological Macromolecules* 311 (2025): 143681.

55. P. G. de Gennes, in *Scaling Concepts in Polymer Physics* (Cornell University Press, 1980).

56. P. J. Flory, "Configurational and Frictional Properties of the Polymer Molecule in Dilute Solution," in *Principles of Polymer Chemistry* (Cornell University Press, 1953), 595.

57. A. R. Maniego, A. T. Sutton, M. Gaborieau, and P. Castignolles, "Assessment of the Branching Quantification in Poly(acrylic acid): Is It as Easy as It Seems?" *Macromolecules* 50 (2017): 9032–9041.

58. Y. C. Yu and W. H. Jo, "Segmented block copolyetheramides based on nylon 6 and polyoxypropylene. I. Synthesis and characterization," *Journal of Applied Polymer Science* 54 (1994): 585–591.

59. M. V. Mokeev and V. V. Zuev, "Rigid phase domain sizes determination for poly(urethane–urea)s by solid-state NMR spectroscopy. Correlation With mechanical properties," *European Polymer Journal* 71 (2015): 372–379.

60. T. Castaing-Cordier, D. Bouillaud, J. Farjon, and P. Giraudeau, "Chapter Four—Recent Advances in Benchtop NMR Spectroscopy and Its Applications," *Annual Reports on NMR Spectroscopy* 103 (2021): 191–258.

61. A. Duchowny and A. Adams, "Compact NMR Spectroscopy for Low-cost Identification and Quantification of PVC Plasticizers," *Molecules (Basel, Switzerland)* 26 (2021): 1221.

62. S. B. Chakrapani, M. J. Minkler, and B. S. Beckingham, "Low-field 1H-NMR Spectroscopy for Compositional Analysis of Multicomponent Polymer Systems," *Analyst* 144 (1679): 1679–1686.

63. K. Singh and B. Blümich, "Compact Low-field NMR Spectroscopy and Chemometrics: A Tool Box for Quality Control of Raw Rubber," *Polymer* 141 (2018): 154–165.

64. J. Tratz, M. Gaborieau, M. Matz, M. Pollard, and M. Wilhelm, "Potential of Benchtop NMR for the Determination of Polymer Molar Masses, Molar Mass Distributions, and Chemical Composition Profiles by Means of Diffusion-Ordered Spectroscopy, DOSY," *Macromolecular Rapid Communications* 45 (2024): 2400512.

65. M. A. Vargas, M. Cudaj, K. Hailu, K. Sachsenheimer, and G. Guthausen, "Online Low-field 1H NMR Spectroscopy: Monitoring of Emulsion Polymerization of Butyl Acrylate," *Macromolecules* 43 (2010): 5561.

66. K. Heerah, S. Waclawek, J. Konzuk, and J. G. Longstaffe, "Benchtop 19F NMR Spectroscopy as a Practical Tool for Testing of Remedial Technologies for the Degradation of Perfluorooctanoic Acid, a Persistent Organic Pollutant," *Magnetic Resonance in Chemistry* 58 (1160): 1160–1167.

67. R. Novoa-Carballal, M. Martin-Pastor, and E. Fernandez-Megia, "Unveiling an NMR-invisible Fraction of Polymers in Solution by Saturation Transfer Difference," *ACS Macro Lett* 10 (1474): 1474–1479.

68. I. Merdas, F. Thominette, and J. Verdu, "Hydrolytic Ageing of Polyamide 11—Effect of Carbon Dioxide on Polyamide 11 Hydrolysis," *Polymer Degradation and Stability* 79 (2003): 419–425.

69. G. Serpe, N. Chaupart, and J. Verdu, "Ageing of Polyamide 11 in Acid Solutions," *Polymer* 38 (1977): 1911–1917.

70. X. Q. Ma, W. L. Xue, Z. X. Zeng, and W. Y. Zhu, "Synthesis and Properties of Polyamide/LLDPE Composites With Compatibilizer Used as Hot Melt Adhesive," *Journal of Adhesion Science and Technology* 30 (2016): 104–116.

71. R. L. Burwell, "The Cleavage of Ethers," *Chemical Reviews* 54 (1954): 615–685.

72. P. Vollhardt and N. Schore, "Reactions of ethers," *Organic Chemistry: Structure and Function* (2011), W.H. Freeman and company, 357.

73. P. Vollhardt and N. Schore, "Reactions of alkenes," *Organic Chemistry: Structure and Function*, 12 (2011), W.H. Freeman and company, 507.

74. J. D. Tanks, M. Kubouchi, and Y. Arao, "Influence of Network Structure on the Degradation of Poly(ether) Amine-cured Epoxy Resins by Inorganic Acid," *Polymer Degradation and Stability* 157 (2018): 153–159.

75. A. Karekar, C. Schicktanz, M. Tariq, et al., "Effects of Artificial Weathering in NR/SBR Elastomer Blends," *Polymer Degradation and Stability* 208 (2023), 110267.

76. P. Castignolles, M. Gaborieau, E. F. Hilder, E. Sprong, C. J. Ferguson, and R. G. Gilbert, "High-Resolution Separation of Oligo(acrylic acid) by Capillary Zone Electrophoresis," *Macromolecular Rapid Communications* 27 (2006): 42–46.

77. N. R. Babij, E. O. McCusker, G. T. Whiteker, et al., "NMR Chemical Shifts of Trace Impurities: Industrially Preferred Solvents Used in Process and Green Chemistry," *Organic Process Research and Development* 20 (2016): 661–667.

78. C. R. Morcombe and K. W. Zilm, "Chemical Shift Referencing in MAS Solid state NMR," *Journal of Magnetic Resonance* 162 (2003): 479–486.

79. M. Gaborieau, T. J. Causon, Y. Guillaneuf, E. F. Hilder, and P. Castignolles, "Molecular Weight and Tacticity of Oligoacrylates by Capillary Electrophoresis-mass Spectrometry," *Australian Journal of Chemistry* 63 (2010): 1219–1226.

80. A. T. Sutton, R. D. Arrua, M. Gaborieau, P. Castignolles, and E. F. Hilder, "Characterization of Oligo(acrylic acid)s and Their Block co-oligomers," *Analytica Chimica Acta* 1032 (2018): 163–177.

81. J. Chamieh, M. Martin, and H. Cottet, "Quantitative Analysis in Capillary Electrophoresis: Transformation of Raw Electropherograms Into Continuous Distributions," *Analytical Chemistry* 87 (2015): 1050–1057.

Supporting Information

Additional supporting information can be found online in the Supporting Information section.

Supporting File: macp70122-sup-0001-SuppMat.pdf